Combined use of alcohol in conventional chemical-induced mouse liver cancer model improves the simulation of clinical characteristics of human hepatocellular carcinoma

BO XIN[1,2*], YING CUI[3*], YANXIA WANG[4*], LEI WANG[5], JIPENG YIN[6],
LICHENG ZHANG[2], HAILIN PANG[1], HELONG ZHANG[1] and RUI-AN WANG[4]

[1]Department of Oncology, Tangdu Hospital, The Fourth Military Medical University, Xi'an, Shaanxi 710038;
[2]Department of Oncology, No. 88 Hospital of People's Liberation Army, Tai'an, Shandong 271000;
[3]Department of Transfusion, Tangdu Hospital, The Fourth Military Medical University, Xi'an, Shaanxi 710038;
[4]Department of Pathology, Xijing Hospital; [5]State Key Laboratory of Cancer Biology, Department of Biochemistry
and Molecular Biology; [6]State Key Laboratory of Cancer Biology, Xijing Hospital of Digestive Diseases,
Xijing Hospital, Fourth Military Medical University, Xi'an, Shaanxi 710032, P.R. China

Abstract. Liver cancer is the one of most common types of cancer and the 2nd cause of cancer-associated mortalities worldwide. Establishing appropriate animal models of liver cancer is essential for basic and translational studies. The present study evaluated the effects of the combined use of alcohol with a conventional chemical-induced mouse liver cancer model. The treatment of alcohol/diethylnitrosamine (DEN)/carbon tetrachloride (CCl_4) in the mice of experimental groups resulted in a series of pathological changes in the liver. Liver inflammation, fibrosis, cirrhosis and hepatocellular carcinoma were identified, and this method used less time (1-5 months) for inducement compared with the conventional chemical-induced method alone. In addition, murine α-fetoprotein (mAFP) was expressed throughout and ultrastructural features met the criteria for liver cancer. Fatty degeneration of pancreas, reduced blood glucose levels, and increased spleen weight were observed. These results indicated that an AFP-secreting hepatocellular carcinoma model of BALB/c mouse was successfully developed. The disease process and morphological changes met the criterion of the liver cancer process. Therefore the model developed in the present study may be an ideal animal model for studying the occurrence and development of liver cancer.

Introduction

Liver cancer is the sixth most common type of cancer and the second leading cause of cancer-associated mortality worldwide, with the highest incidence in Asia and sub-Saharan Africa (1). Hepatocellular carcinoma (HCC) is the most common form of liver cancer, accounting for >90% of cases. HCC affects >700,000 patients per year worldwide and is the most rapidly increasing cause of cancer-associated mortality in developed nations (2). HCC is typically correlated with chronic viral hepatitis infections, particularly hepatitis B or C, aflatoxin B-contaminated dietary intake, alcoholism and metabolic syndrome, including fatty liver disease (3,4). The all-stage survival rate of HCC is 16% and the incidence of HCC is on the rise every year; the incidence rate increased by ~12% from 2006 to 2010 (5). Developing diagnostic and preventive strategies for HCC has been an attractive area for researchers. However, HCC can only be diagnosed at a late stage by currently available serum biomarkers, including α-fetoprotein (AFP) (6), des-γ-carboxy prothrombin and squamous cell carcinoma antigen-immunoglobulin M complexes (7). With the late diagnosis, the five-year survival rate of patients with HCC has been estimated to be very low (5).

Establishing appropriate animal models for HCC is required for basic and translational studies. Several rodent models have been used to study HCC pathogenesis; one of the best experimental systems is the laboratory mouse, owing to the molecular, genetic and physiologic similarities to humans, its breeding capacity, short lifespan and the unlimited options offered by genetic engineering (8).

Since the 1960s, the genotoxic drug diethylnitrosamine (DEN) has been used to induce HCC in rodents (9) and is

Correspondence to: Professor Rui-An Wang, Department of Pathology, Xijing Hospital, Fourth Military Medical University, 169 Changle Road, Xi'an, Shaanxi 710032, P.R. China
E-mail: awangra@fmmu.edu.cn

Professor Helong Zhang, Department of Oncology, Tangdu Hospital, The Fourth Military Medical University, 1 Xinsi Road, Xi'an, Shaanxi 710038, P.R. China
E-mail: cnxazhl@163.com

*Contributed equally

the most widely used chemical to induce liver cancer in mice (8). DEN is the member of the N-nitroso compounds (NOC) family, is considered highly carcinogenic, and has been revealed as a contaminant of beverages, food, tobacco, cosmetic and personal care products among others (8). DEN is a DNA alkylating agent, which can lead to the formation of mutagenic DNA adducts (10). In addition, DEN can generate reactive oxygen species (ROS) following activation by cytochrome P450 (10), which damages DNA, proteins and lipids, and results in cell death. In hepatocytes, DEN is activated by the cytochrome P450 family enzymes (10) and acts as a carcinogen if injected into mice younger than two weeks (when hepatocytes are proliferating) (8). When administered later, tumor-promoting agents may be required (11). The age, sex and genetics of the mice serve roles in the early stages of DEN-induced HCC (12).

Although DEN is the chemical most widely used to induce liver cancer in mice, the commonly used method for using DEN to establish the liver cancer model has limitations: DEN is typically injected into postnatal rats and mice <2 weeks old in order to induce HCC (8), whereas human HCC is typically diagnosed in adults (3). Therefore, although this DEN model is used and considered one of the best chemical models to induce hepatocarcinoma in laboratory rodents, it is not ideal for studying human HCC (13,14). Secondly, when DEN is administered later, tumor-promoting agents are required, for instance: CCl_4, pentobarbital, partial hepatectomy or high fat diet feeding (11,15). Thirdly, these conventional methods require a long period (5-10 months) to induce HCC (13).

Previous research suggests that excessive alcohol use over a prolonged period of time typically results in alcoholic liver disease (ALD), which includes steatosis, steatohepatitis, acute alcoholic steatohepatitis, alcoholic fibrosis and cirrhosis (Laennec's cirrhosis) (16). Multiple pathogenic factors are involved in the development of ALD; alcohol and its metabolites induce reactive oxygen species production and hepatocyte injury through mitochondrial damage and endoplasmic reticulum stress (16). In addition, there is early activation of chemokines, particularly interleukin (IL)8, which contributes to recruitment of neutrophil leukocytes, and monocyte chemoattractant protein-1, which recruits macrophages in the liver (17,18). Activation of Kupffer cells (KCs) has been identified as a central element in the pathogenesis of ALD (19,20). Previous studies have indicated that bacterial endotoxin-lipopolysaccharide (LPS), through Toll-like receptor 4 (TLR4), activate KCs and recruit macrophages in the liver, and that the level of LPS is increased in the portal and the systemic circulation following excessive alcohol intake (21,22). These observations indicate that LPS derived from the gut is a central mediator of inflammation in alcoholic steatohepatitis. Advanced ALD predisposes to hepatocellular cancer; LPS-TLR4 interactions and stem cell Nanog expression serve mechanistic roles in animal models (23,24).

In the present study, an HCC model of adult male BALB/c mouse was induced using the combination of alcohol with a conventional chemical-induced mouse liver cancer model. Induced lesions were subsequently analyzed using histology. The present study aimed to evaluate macroscopic, microscopic and ultrastructural hepatic changes in a BALB/c mouse strain induced by alcohol/DEN/CCl_4, and to report the histological features of pre-neoplastic and neoplastic lesions.

Materials and methods

Animals and experimental conditions. Previous studies have demonstrated that men exhibit higher rates of HCC compared with women, with male:female ratios ranging from 2:1 to 4:1 (14). Therefore, the present study used 80 male mice as subjects. Six-week-old specific pathogen-free BALB/c male mice (20-25 g) were provided by the Animal Center of the Fourth Military Medical University (Xi'an, China) (25). Animals were housed in a specific pathogen-free facility, maintained at a temperature of 23±2˚C, 50±10% humidity, and given free access to water and a regular chow diet, with 14 h light/10 h dark and hardwood bedding. Mice were handled in accordance with institutional guidelines. All animal experiments were approved by the Institutional Animal Care and Use Committee at Fourth Military Medical University (Xi'an, China) and were in accordance with the Declaration of the National Institutes of Health Guide for Care and Use of Laboratory Animals (Publication No. 85-23, revised 1985).

Experimental mouse model procedures. Previous to the present procedures, mice did not receive any treatment. The subsequent quarantine period lasted for one week. At seven weeks of age, 80 mice were identified with ear cuts and randomly divided into 8 groups, as depicted in Fig. 1. On day 1, groups T1, 3, 5 and 7 (experiment groups) were intraperitoneally (i.p.) injected with 100 mg/kg bodyweight of DEN (Sigma-Aldrich; Merck KGaA, Darmstadt, Germany). From day 4, CCl_4 (5 ml/kg, dissolved in olive oil) was administered via gavage twice a week. On day 15, 50 mg/kg bodyweight of DEN was administered via gavage once and 9% alcohol was administered instead of drinking water. From day 22, the dose of CCl_4 was administered up to 8 ml/kg via gavage twice a week. The reason why two different routes were used to administrate DEN is as follows: For higher incidence of HCC, more DEN should be administrated; due to toxicity of DEN and tolerance to DEN/CCl_4 of mice (8). Saline solution was used as a substitute for DEN, CCl_4 and 9% alcohol for groups T2, 4, 6 and 8 (control groups) compared with experiment groups T1, 3, 5 and 7. Mouse weights were noted weekly.

Sample collection and histological processing. On day 60, the first groups (T1 and 2) were sacrificed by means of a lethal i.p. dose of sodium pentobarbital. The remaining groups were sacrificed, correspondingly, at the following days: 90 (T3 and 4), 120 (T5 and 6), 150 (T7 and 8) days following the first DEN injection by the same method mentioned above.

All animals were submitted to necropsies and all macroscopic lesions were recorded. The liver, lungs, spleen, stomach, intestine, pancreas and kidneys were collected and fixed in 10% neutral buffered formalin for 48 h and then samples were routinely processed and paraffin-embedded at room temperature. Relative organ weights were estimated as the ratio of the organ weight to total mouse bodyweight according to Da Costa *et al* (15). Macroscopically visible hepatic nodules were counted and measured using a caliper to determine their largest diameters.

On day 150, macroscopically visible hepatic nodules of T7 and the livers tissues of T8 were diced into 1 mm³ sections, excised and prefixed in 2.5% glutaraldehyde for 3 h at room temperature. Subsequently, post-fixation was performed in cold 1% aqueous osmium tetroxide for 1 h at 4°C. Following rinsing with phosphate buffer, tissue samples were dehydrated in graded ethanol (50, 70, 90 and 100%; 5 min for each) and embedded in Epon 812 for 12 h at room temperature. After sectioning into 50 nm sections, grids were hand stained with 2% uranyl acetate in 50% methanol for 10 min and 1% lead citrate for 7 min at room temperature.

Histological evaluation. Representative histological sections (4 μm-thick) were obtained and stained with hematoxylin and eosin for examination under light microscopy by two different researchers in a blinded fashion and results were compared. Steps of staining with hematoxylin and eosin were as follows and at room temperature: Dewaxing (xylene: I, II, III; 5 min for each), hydrating (ethanol: 100, 95, 90, 80 and 0%; 5 min for each), hematoxylin staining (15 sec), rinsing with water, adding 1% hydrochloric acid alcohol (3-5 sec), eosin staining (2 min), rinsing with water, dehydrating in graded ethanol (70, 90, 95 and 100%; 5 min for each), deparaffinized in xylene (I, II, III; 5 min for each), mounting and coverslipping (neutral balsam).

Images of ultrastructural hepatic tissue samples (T7 and T8) were captured using a JEOL JEM-2000EX transmission electron microscope (JEOL USA, Inc., Peabody, MA, USA).

Reverse transcription-polymerase chain reaction (RT-PCR) analysis. The samples of all experiment groups and T8 (150 days, control group) mice were used to perform RT-PCR analysis. Total RNA was extracted using TRIzol reagent (Invitrogen; Thermo Fisher Scientific, Inc. Waltham, MA, USA), according to the manufacturer's protocol. RNA (1 μg) was reverse transcribed into cDNA according to the instructions of the SuperScript™III Reverse Transcriptase kit (Invitrogen; Thermo Fisher Scientific, Inc.). The PCR primers used were as follows: For mAFP, forward 5'-CTGGCGATG GGTGTTTAG-3' and reverse 5'-TGGTTGTTGCCTGGA GGT-3'; for β-actin, forward 5'-AGTGTGACGTTGACATCC GTA-3' and reverse 5'-CCAGAGCAGTAATCTCCTTCT-3'. The PCR reaction was conducted at 94°C for 5 min, followed by 40 cycles at 94°C for 30 sec, at 56°C for 45 sec and at 72°C for 2 min. PCR was performed using a Bio-Rad iCycler IQ™ 5 (Bio-Rad Laboratories, Inc., Hercules, CA, USA) and Takara Ex Taq® (Takara Bio, Inc., Otsu, Japan), according to the manufacturer's instructions. β-actin was used as endogenous control in this study. PCR products were separated on a 1% agarose gel, and visualized and photographed under ultraviolet light. ImageJ software (1.49n) was used for quantification (National Institutes of Health, Bethesda, MD, USA).

Measurement of blood glucose level. On day 150, the blood glucose levels of group 7 and 8 were measured prior to sacrifice. Blood was collected with a minimum volume (1 μl) from the tail-vein. The glucose level was measured using the Accu-Chek Performa blood glucose monitoring system (glucometer; Roche Diagnostics GmbH, Mannheim, Germany).
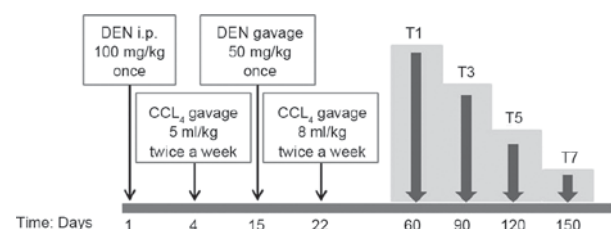

Figure 1. Experimental design. Time is given in weeks post-exposure. Bold arrows indicate time of euthanasia. Saline solution was used as substitutes for DEN, CCl₄ and 9% alcohol for T2, 4, 6 and 8 (control groups) compared to experiment groups T1, 3, 5 and 7. DEN, diethylnitrosamine.

Statistical analysis. Data was analyzed using a two-tailed paired t-test using GraphPad Prism software, version 5.01 (GraphPad Software, Inc., La Jolla, CA, USA). The results are presented as the mean ± standard deviation. $P<0.05$ was considered to indicate a statistically significant difference.

Results

Alcohol/DEN/CCl₄ treatment caused a significant loss of body weight and a significant increase in the liver/body weight ratios of mice. During the experimental protocol, the mortality rate was 7.5% (3/40 mice, one mouse following gavage administration of CCl₄ in T1, and two mice following gavage administration of DEN in T3 and T7) and occurred exclusively in the alcohol/DEN/CCl₄-treated groups. A post-mortem evaluation of animals that succumbed during the experiment was conducted. An anatomic observation of mice that succumbed prematurely during the experiment was made, and the liver, lungs, spleen, stomach, intestine, pancreas and kidneys were collected and observed. Hemorrhage and edema of the intestine and hepatomegaly were observed. Due to male competitive behavior, despite the environmental enrichment, some sporadic injuries associated with the establishment of hierarchy and territory defense were noted, resulting in focal loss of hair (barbering behavior). The liver, lungs, spleen, stomach, intestine, pancreas and kidneys were collected and were carefully examined. The livers and spleens exhibited abnormal changes in weight. Therefore only the changes of liver and spleen are exhibited, and the data of other organs isn't included in the results.

Alcohol/DEN/CCl₄-treated groups demonstrated a significant loss in body weight compared with the control groups on day 30, 60, 90, 120 and 150 ($P<0.05$; Fig. 2A). In addition, the alcohol/DEN/CCl₄-treated mice exhibited a significant increase in liver/body weight ratios compared with the control groups ($P<0.05$ for day 60, $P<0.01$ for day 90, 120 and 150; Fig. 2B).

Macroscopic and microscopic effects of alcohol/DEN/CCl₄ on mouse livers. Exposure to alcohol/DEN/CCl₄ resulted in a sequence of lesions that evolved over time, from chronic toxic lesions observed from T1 (60 days) onwards, fibrosis observed from T3 (90 days), cirrhosis observed from T5 (120 days), to the occurrence of HCC observed from T7 (150 days) (data not shown). Control mice (T2, 4, 6, 8) did not exhibit any significant lesions. T1 (experiment group, 60 days) exhibited
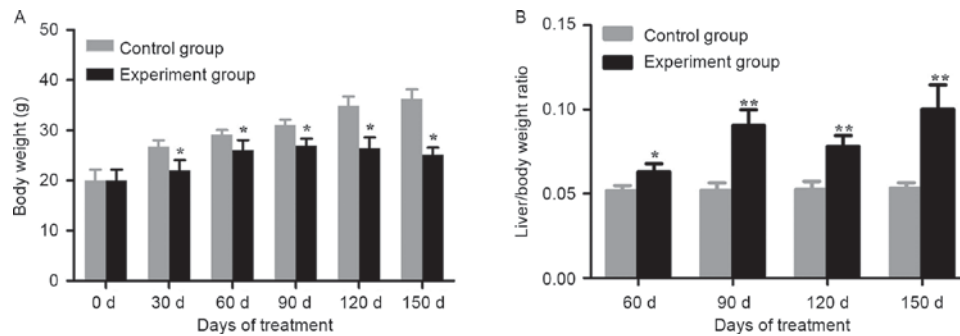
Figure 2. Changes in body weight and the liver/body weight ratios of mice following treatment with DEN. (A) Analysis of the body weight between alcohol/DEN/CCl$_4$-treated mice and the control group (*P<0.05, two-tailed paired t-test). (B) Analysis of the liver/body weight ratio between alcohol/DEN/CCl$_4$-treated mice and the control group (*P<0.05, **P<0.01, two-tailed paired t-test). DEN, diethylnitrosamine.
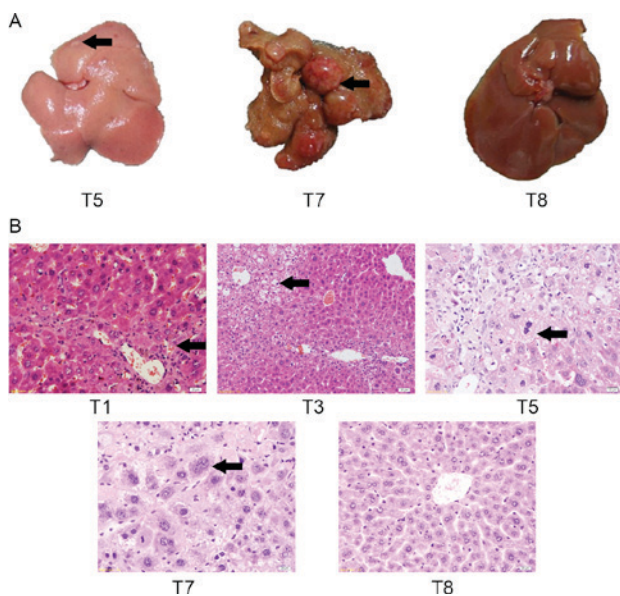

Figure 3. Macroscopic and microscopic features of livers from control and alcohol/DEN/CCl$_4$-treated mice. (A) Note hepatomegally with grey discoloration (arrowhead) and irregular hepatic surface of T5. Note distortion of hepatic lobes, haemorrhagic foci and multiple, grey and yellow nodular lesions (arrowhead) of T7. T8 is the control mouse at 150 days. (B) Hepatitis (DEN-treated mouse at T1), liver fibrosis (DEN-treated mouse at T3), liver cirrhosis (DEN-treated mouse at T5), hepatocellular carcinoma (DEN-treated mouse at T7), normal liver (control mouse at T8). Hematoxylin and eosin staining. Magnification, x400. Time in days (post-treatment): T1: 60 days; T3: 90 days; T5: 120 days; T7/8: 150 days. Scale bar=20 μm. DEN, diethylnitrosamine.

(Department of Pathology, Xijing Hospital, Fourth Military Medical University) in a blinded fashion.

To assess gross changes in liver morphology, macroscopic lesions in liver tissue were identified in T5 and T7 groups, and in the T7 control group (Fig. 3A). At day 150, control mice (T8) did not exhibit any evident hepatic lesions. At day 120, the liver from an alcohol/DEN/CCl$_4$-treated mouse (T5) exhibited an irregular hepatic surface (several small nodules and granular appearance). At day 150, the liver from an alcohol/DEN/CCl$_4$-treated mouse (T7) exhibited multifocal lesions and solitary nodules with a maximum diameter of 10 mm.

Histological hepatic changes of mice in each experiment group were the same (Fig. 3B). Spotty and focal necrosis was identified in liver tissue, and inflammatory cells infiltrated in portal duct areas among mice of the T1 group, which suggested that hepatitis occurred. Lymphocyte and monocyte are a major type of infiltrate in the present study.

Compared with the T1 group, the necrotic area of hepatic lobule, fat droplets of hepatic cells and inflammatory cell infiltration were increased in the T2 group. The dysplasia of connective tissue was observed, but the structure of liver lobule remained normal, which suggested hepatitis increased with appearance of liver fibrosis.

Lobules of liver in the mice of T5 group exhibited a disordered arrangement of hepatocytes and a pile of deposition of fibrous tissue, which suggested the presence of liver cirrhosis. Flipid droplets, hydropic degeneration, necrosis and regeneration of hepatocytes were found. Certain regenerated hepatocytes exhibited a larger volume and binucleate eggs. It is suggested that liver lesions became liver cirrhosis in the present study.

Histologically, the liver lesions of T7 group were classified as the high or middle differentiation group of HCC. These lesions arose within diffuse dysplastic areas, and exhibited invasive growth and a multifocal distribution. The liver lesions were composed of moderately to highly pleomorphic cells disposed in solid nests, trabeculae or multifocal pseudo-acinar structures, supported by a loose fibrovascular stroma. The present study observes that malignant cells were characterized by a large nucleus, an irregular size and shape (pleomorphism), and an irregular border. In addition, malignant cells exhibited a small cytoplasm, frequently with vacuoles and consequently exhibit an increased nuclear-cytoplasmic (N/C) ratio. Some tumor giant cells and irregular mitosis were observed.

hepatitis (90%, one succumbed following gavage administration of CCl$_4$), T3 (experiment group, 90 days) exhibited liver fibrosis (90%, one succumbed following gavage administration of DEN), T5 (experiment group, 120 days) exhibited liver cirrhosis (100%), T7 (experiment group, 150 days) exhibited high or middle differentiation group of HCC (90%, one succumbed following gavage administration of DEN), which means that the malignant transformation rate of the surviving mice in T7 (experimental group, 150 days) was 100% and the liver lesions were classified as the high or middle differentiation group of HCC according to the International Classification of Rodent Tumors and the update on precursors and early lesion on HCC (15) under light microscopy by two pathologists

Changes in ultrastructure and mAFP in alcohol/DEN/CCl₄-treated and control mice livers. Electron microscopy revealed specific ultrastructural changes in hepatic cells under experimental conditions. Examples of a normal hepatic cell from group T8 and a malignant hepatic cell of group T7, and their organelles are illustrated in Fig. 4A. The hepatocytes of group T8 were polygonal, with oval-shaped nuclei in the center accompanied by more euchromatin and less heterochromatin. The cytoplasm was crowded with mitochondria, rough and smooth endoplasmic reticulum, golgi apparatus, ribosomes and glycogen particles. The lumen of the cholangioles were filled with numerous microvilli of hepatocytes.

Malignant cells of group T7 were characterized by a large nucleus and a small cytoplasmic amount resulting in an increased N/C ratio; the mitochondrial structure was loose and vacuolated, and certain mitochondrial cristae were broken or absent; the cholangioles exhibited poor development, which resulted in cholestasis and less microvilli (arrowhead).

The expression of mAFP in liver tissues of alcohol/DEN/CCl₄-treated and control mice was examined. Liver inflammation, fibrosis, cirrhosis and hepatocellular carcinoma can cause AFP elevation compared with normal liver (26). The expression of AFP mRNA detected by RT-PCR was used to test whether AFP was expressed during the whole experimental process following treatment with alcohol/DEN/CCl₄. The mAFP expression in the liver tissues of treated mice was significantly increased compared with that in control mice, as determined by RT-PCR ($P<0.05$; Fig. 4B).

Changes in other internal organs in alcohol/DEN/CCl₄-treated and control mice. The lungs, spleen, stomach, intestine, pancreas and kidneys were collected and were carefully examined. Only the spleen and pancreas exhibited abnormal changes in histology or weight. The pancreas of control mice at T8 exhibited normal architecture and cells; however, the pancreas of DEN-treated mouse at T3 (90 days), T5 (120 days), and T7 (150 days) exhibited sporadic hydropic degeneration (arrowhead), mild hydropic degeneration (larger size but lower degree, arrowhead) or moderate hydropic degeneration (arrowhead), respectively (Fig. 5A).

On day 150, the alcohol/DEN/CCl₄-treated mice of T7 exhibited a decreased blood glucose level ($P<0.05$; Fig. 5B), but a significant increase in spleen weight ($P<0.01$; Fig. 5C) and spleen/body weight ratios ($P<0.01$; Fig. 5D) compared with control mice of T8 at 150 days.

Discussion

The present study aimed to evaluate the macroscopic, microscopic and ultrastructural hepatic changes induced by alcohol/DEN/CCl₄ in adult male BALB/c mice, which is a novel method of inducing liver cancer in a mouse model.

The genotoxic drug DEN is the most widely used chemical to induce liver cancer in mice (8). In the model of the present study, HCC development is similar to that in patients and typically follows a slow multistep sequence, in which cycles of necrosis and regeneration promote neoplastic transformation (8,11,15). The progression from early dysplastic lesions to fully malignant tumors is associated with an increased
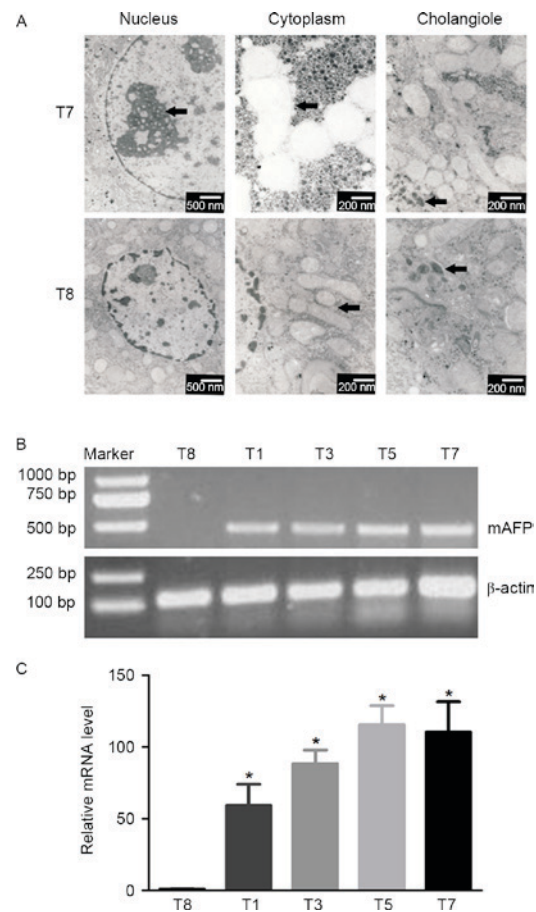

Figure 4. Ultrastructural hepatic changes and mAFP level in alcohol/DEN/CCl₄-treated and control mice livers. (A) Note abnormal and normal ultrastructural hepatic changes of T7/8. Different effects of nucleus (arrowhead, bar=500 nm), cytoplasm (arrowhead, scale bar=200 nm), and cholangiole (arrowhead, scale bar=500 nm) were observed. (B) Liver tissues of alcohol/DEN/CCl₄-treated mice exhibited increased mAFP mRNA levels compared with control mice. (C) Analysis of the mAFP mRNA level between alcohol/DEN/CCl₄-treated mice and the control group (*$P<0.05$, two-tailed paired t-test). Time in days (post-treatment): T1: 60 days; T3: 90 days; T5: 120 days; T7/8: 150 days. DEN, diethylnitrosamine; mAFP, mouse α-fetoprotein.

occurrence of genomic alterations (10,27,28). The similarities and differences between the model of the present study and the conventional one (DEN + phenoparpital) are that DEN and phenoparpital were typically used in postnatal rats and mice younger than 2 weeks for inducing HCC, whereas DEN/CCl₄/alcohol in the present study were used in adult mice older than 7 weeks. DEN and phenoparpital takes 6-9 months to induce HCC, whereas DEN/CCl₄/alcohol in the present study took 5 months to induce HCC (29).

CCl₄ is a tumor-promoting agent that is typically associated with classic experimental models for steatohepatitis and liver fibrosis (8). If used for the HCC model, CCl₄ may be used for >12 months and is typically combined with DEN or genetic models (8). The mechanism involves the generation of free radicals during CCl₄ metabolism by cellular cytochrome P450 in the liver, including trichloromethyl and oxygen-centered lipid radicals, which result in lipid peroxidation, DNA modification, mitochondrial damage and even cell death (30).

Alcohol is associated with HCC via the development of cirrhosis; however, the published evidence does not support
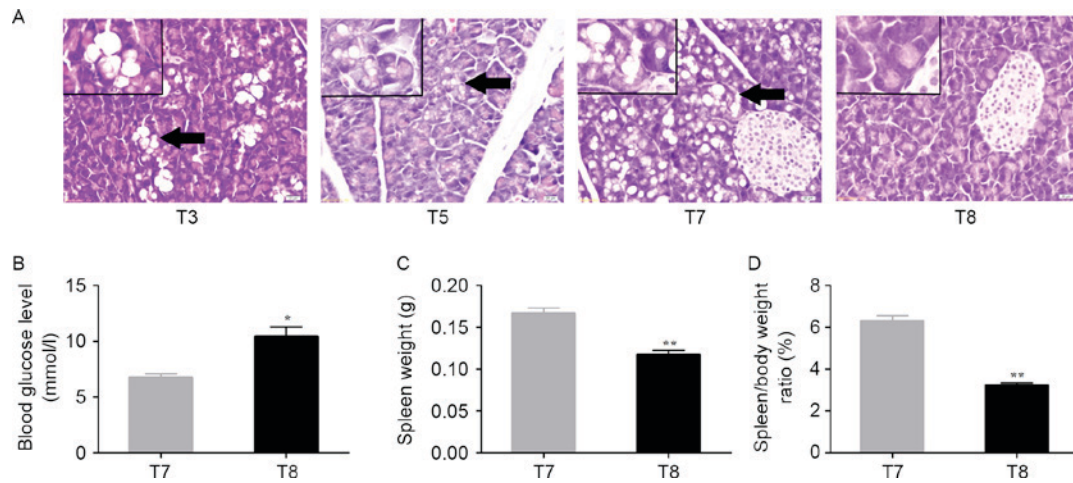
Figure 5. Changes in pancreas and spleen in alcohol/DEN/CCl₄-treated and control mice. (A) Histological pancreatic changes in alcohol/DEN/CCl₄-treated and control mice. The pancreas of control mice at T8 exhibited normal architecture and cells. The pancreas of DEN-treated mouse at T3 (90 days), T5 (120 days), and T7 (150 days) exhibited a sporadic hydropic degeneration (arrowhead), mild hydropic degeneration (bigger size but lower degree, arrowhead), or moderate hydropic degeneration (arrowhead) respectively. Hematoxylin and eosin staining. Magnification, x400. Scale bar=20 μm. (B) Analysis of blood glucose levels between treated and control mice at 150d (*P<0.05, a two-tailed paired t-test). (C) Analysis of spleen weight between treated and control mice at day 150 (**P<0.01, a two-tailed paired t-test). (D) Analysis of spleen/body weight ratio (%) between treated and control mice at 150 days (**P<0.01, a two-tailed paired t-test). Time in days (post-treatment): T3: 90 days; T5: 120 days; T7/8: 150 days. DEN, diethylnitrosamine.

a role for alcohol as a direct carcinogen for HCC (31). The mechanism of alcohol-induced hepatotoxicity includes interactions between the direct toxic effects and alcohol metabolites on various cell types in the liver, induction of reactive oxygen species, upregulation of the inflammatory cascade, in addition to other cell-specific effects in the liver (32).

DEN is a chemical carcinogenic agent, and CCl₄ and alcohol are tumor-promoting agents (8). By using chemical carcinogenic agents and tumor-promoting agents together, the present study developed an AFP-secreting HCC model in the BALB/c mouse.

The findings of the present study are similar to those of Da Costa *et al* (15), who observed that DEN-induced hepatic lesions in mice, from initial lesions to malignant neoplasms. However, the present study presented some differences from their studies. At day 150, following the first DEN injection (T7, 150 days following first DEN exposure), an AFP-secreting HCC model developed faster compared with just using DEN, by using adult mice not postnatal mice. The malignant transformation rate of the survival mice in experimental groups was 100%, and the liver lesions were classified as the high or middle differentiation group of HCC. These lesions arose within diffuse dysplastic areas, and exhibited invasive growth and a multifocal distribution. The ultrastructural changes of the induced liver neoplasms model were similar to those of human liver cancer (8). Fatty degeneration was observed in the pancreas, and the blood glucose levels were reduced compared with the control, which may be similar to paraneoplastic syndrome (PNS) in humans (31). In addition to liver dysfunction, the histological changes in the pancreas may account for why the blood glucose levels were reduced. The treated mice demonstrated a significant increase in spleen weight and spleen/body weight ratios compared with control mice at day 150, which may be similar to spleen changes in humans when HCC occurs (31).

The present study had certain limitations. The sample size was relatively small. The changes of liver lesion's ultrastructure,

blood glucose level and spleen weight were observed only at day 150. The level of insulin was not detected. Although there is previously published research concerning the DEN-only group (15), the DEN-only group was not selected as a control for comparison. In future, studies including all the relevant controls for models of HCC induction are required in order to confirm these preliminary observations. The reasons for the ultrastructure and measurement of blood glucose level only being performed at 150 days following treatment is that the lobules of liver in the mice of T5 group (120 days) were observed to exhibit a disordered arrangement of hepatocytes and a pile of deposition of fibrous tissue, which suggested liver cirrhosis. Therefore, changes in ultrastructure in the T7 groups (150 days) were detected to confirm the presence of HCC. The present study aimed to detect changes in pancreatic structure; however, the pancreases of DEN-treated mice at T3 (90 days) and T5 (120 days) exhibited sporadic hydropic degeneration or mild hydropic degeneration, respectively. It would have been appropriate to investigate whether changes in structure could cause changes in blood glucose level; however, the whole blood of mice had not been preserved. In future studies, the results of this preliminary study would be further confirmed with complete haematological studies, analyzing the levels of liver biomarkers such as alanine transaminase, bilirubin, albumin and alkaline phosphatase, and improved pathohistological methods and quantification of AFP at the mRNA (RT-quantitative PCR) and protein (ELISA, immunohistochemistry) level.

In conclusion, the present study used chemical carcinogenic agents and tumor-promoting agents together to successfully develop an AFP-secreting HCC model in adult male BALB/c mouse for the first time, to the best of our knowledge. This method used less time for inducement and the malignant transformation rate of the surviving mice in the experimental groups was 100%. The disease process and ultrastructural changes met the criterion of the human liver cancer process (2). In addition, the changes of blood glucose levels

were similar to PNS in humans and the increase in spleen weight was similar to spleen changes during human HCC (31). Therefore, this model may be an ideal experimental animal model for studying the occurrence and development of liver cancer, and may be a novel animal model for studying PNS in primary hepatic carcinoma.

Acknowledgements

References

1. Nordenstedt H, White DL and El-Serag HB: The changing pattern of epidemiology in hepatocellular carcinoma. Dig Liver Dis 42 (Suppl 3): S206-S214, 2010.
2. Dhanasekaran R, Limaye A and Cabrera R: Hepatocellular carcinoma: Current trends in worldwide epidemiology, risk factors, diagnosis, and therapeutics. Hepat Med 4: 19-37, 2012.
3. Kassebaum NJ, Bertozzi-Villa A, Coggeshall MS, Shackelford KA, Steiner C, Heuton KR, Gonzalez-Medina D, Barber R, Huynh C, Dicker D, et al: Global, regional, and national levels and causes of maternal mortality during 1990-2013: A systematic analysis for the Global Burden of Disease Study 2013. Lancet 384: 980-1004, 2014.
4. Calle EE, Rodriguez C, Walker-Thurmond K and Thun MJ: Overweight, obesity, and mortality from cancer in a prospectively studied cohort of U.S. adults. N Engl J Med 348: 1625-1638, 2003.
5. Siegel R, Ma J, Zou Z and Jemal A: Cancer statistics, 2014. CA Cancer J Clin 64: 9-29, 2014.
6. Sherman M: The resurrection of alphafetoprotein. J hepatol 52: 939-940, 2010.
7. Bertino G, Neri S, Bruno CM, Ardiri AM, Calvagno GS, Malaguarnera M, Toro A, Malaguarnera M, Clementi S, Bertino N and Di Carlo I: Diagnostic and prognostic value of alpha-fetoprotein, des-γ-carboxy prothrombin and squamous cell carcinoma antigen immunoglobulin M complexes in hepatocellular carcinoma. Minerva Med 102: 363-371, 2011.
8. Bakiri L and Wagner EF: Mouse models for liver cancer. Mol Oncol 7: 206-223, 2013.
9. Rajewsky MF, Dauber W and Frankenberg H: Liver carcinogenesis by diethylnitrosamine in the rat. Science 152: 83-85, 1966.
10. Qi Y, Chen X, Chan CY, Li D, Yuan C, Yu F, Lin MC, Yew DT, Kung HF and Lai L: Two-dimensional differential gel electrophoresis/analysis of diethylnitrosamine induced rat hepatocellular carcinoma. Int J Cancer 122: 2682-2688, 2008.
11. Park EJ, Lee JH, Yu GY, He G, Ali SR, Holzer RG, Osterreicher CH, Takahashi H and Karin M: Dietary and genetic obesity promote liver inflammation and tumorigenesis by enhancing IL-6 and TNF expression. Cell 140: 197-208, 2010.
12. Diwan BA, Rice JM, Ohshima M and Ward JM: Interstrain differences in susceptibility to liver carcinogenesis initiated by N-nitrosodiethylamine and its promotion by phenobarbital in C57BL/6NCr, C3H/HeNCrMTV- and DBA/2NCr mice. Carcinogenesis 7: 215-220, 1986.
13. Pok S, Wen V, Shackel N, Alsop A, Pyakurel P, Fahrer A, Farrell GC and Teoh NC: Cyclin E facilitates dysplastic hepatocytes to bypass G1/S checkpoint in hepatocarcinogenesis. J Gastroenterol Hepatol 28: 1545-1554, 2013.
14. Wong VW and Janssen HL: Can we use HCC risk scores to individualize surveillance in chronic hepatitis B infection? J Hepatol 63: 722-732, 2015.
15. Da Costa RM, Paula-Santos N, Rocha AF, Colaco A, Lopes C and Oliveira PA: The N-nitrosodiethylamine mouse model: Sketching a timeline of evolution of chemically-induced hepatic lesions. Anticancer Res 34: 7029-7037, 2014.
16. Szabo G: Gut-liver axis in alcoholic liver disease. Gastroenterology 148: 30-36, 2015.
17. Mandrekar P, Ambade A, Lim A, Szabo G and Catalano D: An essential role for monocyte chemoattractant protein-1 in alcoholic liver injury: Regulation of proinflammatory cytokines and hepatic steatosis in mice. Hepatology 54: 2185-2197, 2011.
18. Szabo G, Petrasek J and Bala S: Innate immunity and alcoholic liver disease. Dig Dis 30 (Suppl 1): S55-S60, 2012.
19. Wheeler MD, Kono H, Yin M, Nakagami M, Uesugi T, Arteel GE, Gäbele E, Rusyn I, Yamashina S, Froh M, et al: The role of Kupffer cell oxidant production in early ethanol-induced liver disease. Free Radic Biol Med 31: 1544-1549, 2001.
20. Enomoto N, Ikejima K, Bradford BU, Rivera CA, Kono H, Goto M, Yamashina S, Schemmer P, Kitamura T, Oide H, et al: Role of Kupffer cells and gut-derived endotoxins in alcoholic liver injury. J Gastroenterol Hepatol 15 (Suppl): D20-D25, 2000.
21. Uesugi T, Froh M, Arteel GE, Bradford BU and Thurman RG: Toll-like receptor 4 is involved in the mechanism of early alcohol-induced liver injury in mice. Hepatology 34: 101-108, 2001.
22. Petrasek J, Mandrekar P and Szabo G: Toll-like receptors in the pathogenesis of alcoholic liver disease. Gastroenterol Res Pract 2010: pii:710381, 2010.
23. Dapito DH, Mencin A, Gwak GY, Pradere JP, Jang MK, Mederacke I, Caviglia JM, Khiabanian H, Adeyemi A, Bataller R, et al: Promotion of hepatocellular carcinoma by the intestinal microbiota and TLR4. Cancer Cell 21: 504-516, 2012.
24. Machida K, Tsukamoto H, Mkrtchyan H, Duan L, Dynnyk A, Liu HM, Asahina K, Govindarajan S, Ray R, Ou JH, et al: Toll-like receptor 4 mediates synergism between alcohol and HCV in hepatic oncogenesis involving stem cell marker Nanog. Proc Natl Acad Sci USA 106: 1548-1553, 2009.
25. Kapanadze T, Gamrekelashvili J, Ma C, Chan C, Zhao F, Hewitt S, Zender L, Kapoor V, Felsher DW, Manns MP, et al: Regulation of accumulation and function of myeloid derived suppressor cells in different murine models of hepatocellular carcinoma. J Hepatol 59: 1007-1013, 2013.
26. El-Serag HB, Kanwal F, Davila JA, Kramer J and Richardson P: A new laboratory-based algorithm to predict development of hepatocellular carcinoma in patients with hepatitis C and cirrhosis. Gastroenterology 146: 1249-1255.e1, 2014.
27. Farazi PA and DePinho RA: Hepatocellular carcinoma pathogenesis: From genes to environment. Nat Rev Cancer 6: 674-687, 2006.
28. Thorgeirsson SS and Grisham JW: Molecular pathogenesis of human hepatocellular carcinoma. Nat Genet 31: 339-346, 2002.
29. Teufel A, Maass T, Strand S, Kanzler S, Galante T, Becker K, Strand D, Biesterfeld S, Westphal H and Galle PR: Liver-specific Ldb1 deletion results in enhanced liver cancer development. J Hepatol 53: 1078-1084, 2010.
30. Cai Z, Lou Q, Wang F, Li E, Sun J, Fang H, Xi J and Ju L: N-acetylcysteine protects against liver injure induced by carbon tetrachloride via activation of the Nrf2/HO-1 pathway. Int J Clin Exp Pathol 8: 8655-8662, 2015.
31. Saran U, Humar B, Kolly P and Dufour JF: Hepatocellular Carcinoma and Lifestyles. J Hepatol 64: 203-214, 2016.
32. Neuman MG, Maor Y, Nanau RM, Melzer E, Mell H, Opris M, Cohen L and Malnick S: Alcoholic liver disease: Role of cytokines. Biomolecules 5: 2023-2034, 2015.